

## Correlation-potential method for negative ions and electron scattering

V. A. Dzuba<sup>1,2</sup> and G. F. Gribakin<sup>1</sup>

<sup>1</sup>*School of Physics, University of New South Wales, Kensington, New South Wales 2033, Australia*

<sup>2</sup>*Institute of Semiconductor Physics, 630090 Novosibirsk, Russia*

(Received 15 October 1993)

The relativistic correlation-potential method was used to calculate binding energies and fine-structure intervals for Pd, Ba, and Yb negative ions and to investigate low-energy electron scattering by Yb, Hg, and Ra atoms. The results for the binding energies are the following: 540 meV for the  $5s$  state of  $\text{Pd}^-$ , 190 and 133 meV for the  $6p_{1/2}$  and  $6p_{3/2}$  states of  $\text{Ba}^-$ , and 36 meV for the  $6p_{1/2}$  state of the  $\text{Yb}^-$ . A number of prominent  $p$  and  $d$  resonances are revealed in the scattering phase-shift calculations. These  $p$  or  $d$  resonances lead to a phenomenon of 100% polarization of the scattered electron beam at appropriate electron energy and scattering angle. A criterion is proposed to measure the strength of the nonlocal correlation potential and to evaluate its ability to create a bound state:  $\int G(r', r) \Sigma(r, r') dr dr' > 1$  is the necessary condition for the formation of a bound state. Here  $\Sigma$  is the correlation potential and  $G$  is the electron Green's function at zero energy.

PACS number(s): 31.20.Tz, 34.80.Bm, 34.80.Nz, 03.65.Ge

### I. INTRODUCTION

A number of calculations of electron affinities for alkaline-earth-metal atoms have been carried out since the first prediction [1] and discovery [2] of  $\text{Ca}^-$ —the first negative ion of this series [3–10]. It has been shown that all heavy atoms of the Ca group (Ca, Sr, Ba, and Ra) have stable negative ions with  $ns^2np$  configuration. The existence of  $\text{Sr}^-$  and  $\text{Ba}^-$  ions was confirmed experimentally by means of accelerator mass spectrometry [11]. The previously accepted view that alkaline-earth elements cannot form stable negative ions because of their closed subshell structure was completely disproved by both theoretical and experimental investigations.

There are two other atoms with closed subshells which have stable negative ions—Pd and Yb, according to experimental observations [12,13] and a number of calculations [3,8,14,15]. The six atoms mentioned above apparently exhaust the number of closed-shell atoms capable of forming negative ions. They have this property due to a strong correlation interaction between the atom and the electron, which can be related to the large dipole polarizability of the atom. All other closed-shell atoms have relatively small static dipole polarizabilities, which means that their interaction with an extra electron is too weak to form a bound state.

In spite of strong evidence for the negative ions' existence, both experimental and theoretical data are far from being complete yet. The electron affinity was measured for only two atoms of the six: Pd [12] and Ca [2]. As for the Sr, Ba, and Yb, the corresponding negative ions were observed [11,13], but none of the electron affinities had been measured. Most of the electron-affinity calculations for atoms of this type were made for the ground state only, and some of them were nonrelativistic. However, as was shown in [10] and [14], the relativistic effects are very important. The  $p$  bound states of these nega-

tive ions have large fine structure, which is comparable in magnitude with the electron affinity and for Ra [10] and Yb [14] is even larger than the affinity. In both of these atoms  $p_{3/2}$  states are revealed as resonances in the continuum. It gives rise to a phenomenon of a 100% spin polarization of the scattered electron beam at appropriate electron energy and scattering angle [16]. Calculations of the electron-beam polarization were done in [16] for the  $p$  resonance in Ra and the  $d$  resonance in Ba. The same effect occurs for the  $p$  resonance in Yb (see below). It may seem that from an experimental point of view these atoms are not the best system in which to observe this phenomenon. As will be discussed below the only thing one needs to produce 100% polarization of the scattered electron beam is a distinct  $p$ -wave resonance in electron scattering from a heavy atom. From this point of view the Hg atom seems to be a very good candidate to observe the phenomenon, as it indeed has a low-energy  $p$ -wave resonance [17]. Note here that the spin polarization has been calculated by Yuan and Zhang [18] in the model potential approach for lighter atoms of the Hg group (Mg, Zn, and Cd), where the polarization did not reach 100% because of the smaller relativistic effects, and for Ba [19], where the results at low energy are similar to [16].

As was mentioned above, the formation of negative ions by closed-shell atoms is caused by the correlation interaction of the extra electron with the neutral atom. At large distances this nonlocal energy-dependent interaction turns into a local polarization potential of the form  $-\alpha e^2/2r^4$  where  $\alpha$  is the electric-dipole polarizability of the atom. Therefore, in general  $\alpha$  may be considered as a measure of the correlation potential strength. It is very important to have such a measure, because if the value of the polarizability is known, it gives a hint as to whether the negative-ion state is bound or not prior to calculations. On the other hand, the magnitude of  $\alpha$  gives only very approximate information. There is no critical value

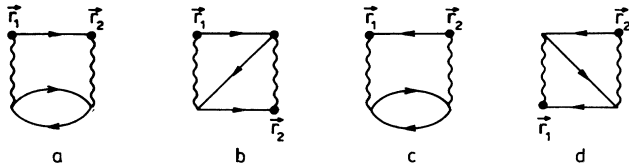


FIG. 1. Second-order correlation diagrams in hole-particle presentation.

of  $\alpha$  beyond which one could be sure that the correlation interaction is strong enough to form a negative ion. Thus the Pd atom has smaller polarizability than Zn, Cd, and Hg atoms, yet it forms a negative ion while the others do not. When a bound state is expected,  $\alpha$  does not tell what type of symmetry it should be. For example, in the first unsuccessful attempts to calculate the binding energy of the  $\text{Yb}^-$  ion the  $6s^25d$  configuration was considered [20], while, as was shown in later works [14,15], it should actually be of the  $6s^26p$  configuration. And finally, the value of the polarizability does not provide any information about the correlation interaction at small distances. If we adopt a many-body diagrammatic approach, the correlation interaction in the second order of the perturbation theory in the residual Coulomb interaction is described by the four diagrams presented in Fig. 1. Only one of them (a) contributes to the long-range local polarization potential, which is proportional to the polarizability. But it is known that the other diagrams, and the exchange diagram [(b) in Fig. 1] in particular are important and should be taken into account to obtain the correct result for the binding energy. They contribute to the correlation interaction at small distances where the asymptotic formula is not valid, and where  $\alpha$  cannot serve as a measure of the correlation interaction strength.

In the present paper we propose a numerical criterion for the strength of the nonlocal correlation potential. It accounts for both long-range and short-range behavior of the correlation potential and is applicable to each partial wave separately. It has the form of a necessary condition, so that if its value is less than 1, then the correlation potential is too weak to form a bound state of a given symmetry. The proposed criterion generalizes the well-known Bargman criterion [21] to the case of a nonlocal correlation potential acting on a background of zero order, e.g., Hartree-Fock, potential. Using the criterion one can examine the contribution of each of the four diagrams to the correlation potential.

## II. METHOD OF CALCULATION

To calculate the scattering phase shifts or the binding energy for the external electron interacting with a closed-shell atom we use the correlation-potential method which was described in our earlier works [10,16,22,23]. We briefly repeat it here with some necessary comments. The electron wave function is found from the single-particle equation (the application of the nonrelativistic Dyson equation to negative ions was proposed in [3]):

$$(\hat{H}_0 + \hat{\Sigma})\psi_a = E_a\psi_a, \quad (1)$$

where  $\hat{H}_0$  is the relativistic Hartree-Fock-Dirac Hamiltonian

$$\hat{H}_0 = c\vec{\alpha} \cdot \mathbf{p} + (\beta - 1)mc^2 - \frac{Ze^2}{r} + \hat{V}^N, \quad (2)$$

$\hat{V}^N = \hat{V}_{\text{dir}} + \hat{V}_{\text{exch}}$  is the sum of the direct and nonlocal exchange Hartree-Fock potentials created by  $N$  electrons of the neutral atom, and  $\hat{\Sigma}$  is the nonlocal correlation potential which describes the correlation interaction of the external electron with the neutral atom. The calculation of  $\hat{\Sigma}$  will be discussed below. Similar to  $\hat{V}_{\text{exch}}$ ,  $\hat{\Sigma}$  is an integral operator:

$$\hat{\Sigma}\psi_a = \int \Sigma(\mathbf{r}_1, \mathbf{r}_2, E_a)\psi(\mathbf{r}_2)d^3r_2, \quad (3)$$

and can be taken into account in a similar manner when solving (1). We solve (1) iteratively, starting from the Hartree-Fock continuous spectrum wave function for the electron scattering problem. As far as the calculation of the negative-ion bound state is concerned, it is impossible to consider  $\hat{\Sigma}$  as a perturbation since there is no binding at all if  $\hat{\Sigma}$  is neglected. So, one needs an appropriate initial approximation  $\psi_0$  to solve (1) iteratively. We calculate  $\psi_0$  in the potential

$$\hat{V} = \hat{V}^N + \delta V, \quad \text{where } \delta V = \begin{cases} -e^2/r_0, & r < r_0 \\ -e^2/r, & r \geq r_0, \end{cases} \quad (4)$$

$r_0$  is a fit parameter which is chosen to obtain rapid convergence. Then (1) is solved, providing the energy and the wave function for the outer electron in the negative ion.

### A. Calculation of $\hat{\Sigma}$

The correlation potential  $\hat{\Sigma}$  in the lowest, second order in the residual Coulomb interaction, is described by four diagrams shown in Fig. 1. The direct diagrams 1(a) and 1(c) usually dominate over the exchange diagrams 1(b) and 1(d), respectively, and we use different techniques to calculate them. The direct diagrams are calculated using Green's functions and the Feynman diagram technique. It enables one to calculate an infinite series of higher-order diagrams which account for the screening of the Coulomb interaction and to take into account the hole-particle interaction in the polarization operator [the loops in Figs. 1(a) and 1(c)]. It also provides better numerical accuracy than direct summation over the intermediate states. The diagrams 1(a) and 1(c) correspond to the Feynman type diagram in Fig. 2(a), while the exchange diagrams 1(b) and 1(d) correspond to the diagram 2(b). The evaluation of the exchange diagram 2(b) in the Feynman technique is much more complicated than for the direct one because of the double integration over the intermediate energies. On the other hand, the

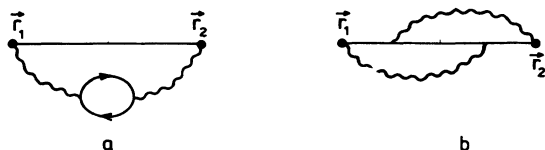


FIG. 2. Second-order diagrams for  $\hat{\Sigma}$  in Feynman diagram technique.

contribution of the exchange diagram is usually several times smaller than the direct one. Thus we do not need such a high accuracy in the calculation of the exchange diagrams and we calculate it by means of direct summation over the intermediate states. The higher-order corrections to them can be taken into account in an approximate way by introducing the screening factors  $f_k$  in each Coulomb line ( $k$  is the multipolarity of the Coulomb interaction). The values of  $f_k$  can be estimated from accurate calculations of the higher-order correlations to the direct diagram.

There are two classes of higher-order diagrams important for the correlation potential  $\hat{\Sigma}$ : the particle-hole interaction in the polarization operator (Fig. 3), and the screening of the electron-electron interaction (Fig. 4). For the outer electron in the neutral Cs atom their relative contribution is about 20–40% of the total correlation correction to the energy level. However, it turns out that they strongly compensate each other, so that the resulting correction is small. Nevertheless, taking into account the higher-order corrections in the Cs atom substantially improves the agreement between the calculated and the experimental data for both the energy levels and the fine-structure intervals [23]. It is a surprising fact that for the negative ions the cancellation between these two classes of higher-order diagrams is even closer. They change the energy of the  $4p_{1/2}$  bound state of  $\text{Ca}^-$  by only 15.2 meV, but hardly change the fine-structure interval [10]. We checked this for  $\text{Pd}^-$  as well. If the correlation potential  $\hat{\Sigma}$  is calculated in the second order in the residual Coulomb interaction, the binding energy of the  $5s$  state of  $\text{Pd}^-$  is 540 meV. But when we take into account the hole-particle interaction and the screening of the Coulomb interaction it becomes 520 meV, i.e., changes very little. Note that the second order value 540 meV is in better agreement with the experimental value of 560 meV [12]. We encountered a similar situation for the  $\text{Ca}^-$ : though the higher-order corrections increase the binding energy of  $\text{Ca}^-$ , the second-order value is also closer to the experimental one [10]. Note that the electron affinity is extremely sensitive to the magnitude of the correlation potential because most of its strength is responsible for the electron binding itself and only a rela-

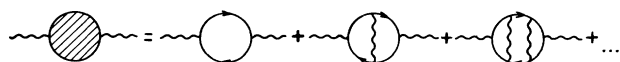


FIG. 3. Hole-particle interaction in the polarization operator.



FIG. 4. Screening of the electron-electron interaction.

tively small fraction of it deepens the level to the position observed. The smaller the value of the electron affinity, the more sensitive it is to the accuracy of the correlation potential calculation. So, as one cannot hope to systematically improve the results by calculation of higher-order diagrams, we will use the second-order approximation for  $\hat{\Sigma}$ . It corresponds to an accuracy of several percent in  $\hat{\Sigma}$ , that in turn corresponds to an accuracy of about 10% in the binding energy of  $\text{Pd}^-$  and about 40% in the binding energy of  $\text{Yb}^-$ .

### B. Electric-dipole polarizabilities

The dipole polarizability of the atom  $\alpha$  determines the long-range asymptotic behavior of the correlation potential  $\hat{\Sigma}$ :

$$\Sigma(\mathbf{r}_1, \mathbf{r}_2, E_\alpha) \rightarrow -\frac{\alpha e^2}{2r_1^4} \delta(\mathbf{r}_1 - \mathbf{r}_2). \quad (5)$$

The values of  $\alpha$  for the Pd, Ba, Yb, Hg, and Ra atoms, calculated from the second order  $\hat{\Sigma}$  are presented in Table I. On the whole they are slightly smaller than the recommended ones from [24], although, in many cases they fall within the given uncertainty. We checked that accounting for the hole-particle interaction and screening improves the agreement. For example, for the Yb atom it increases  $\alpha$  from 125 a.u. to 135 a.u. There is again a close cancellation between the two classes of higher-order diagrams: when only the screening is included the value of  $\alpha$  drops down to 77 a.u. On the other hand the polarizability of Pd, estimated at 18.7 a.u., is close to what is obtained from the random phase approximation [25]. Therefore, we suppose that the recommended value of  $\alpha$  for Pd is overestimated.

It is worth stressing once more that a proper value of  $\alpha$  is only a relative measure of the correlation-potential strength. We believe that good agreement between calculated and measured electron affinities is more important, and it justifies neglecting higher-order corrections to  $\hat{\Sigma}$ .

TABLE I. Electric-dipole polarizabilities of atoms (a.u.).

| Atom | Present paper | Recommended values [24] | Others           |
|------|---------------|-------------------------|------------------|
| Pd   | 18.7          | $32 \pm 8$              | 22 <sup>a</sup>  |
| Ba   | 220           | $268 \pm 21$            |                  |
| Yb   | 125           | $142 \pm 36$            | 205 <sup>b</sup> |
| Hg   | 41.2          | $38 \pm 10$             | 34 <sup>c</sup>  |
| Ra   | 205           | $258 \pm 65$            |                  |

<sup>a</sup>RPAE approximation [25].

<sup>b</sup>Gribakina *et al.* [15].

<sup>c</sup>Reference [26].

### C. Criterion for the strength of the correlation potential

If the correlation potential  $\hat{\Sigma}$  is strong enough to form a bound state of a given symmetry, it must satisfy the following condition (see the Appendix):

$$g_{\kappa} = \int G_{\kappa}(r', r) \Sigma_{\kappa}(r, r') dr dr' > 1, \quad (6)$$

where  $\kappa = (-1)^{(l+j+\frac{1}{2})} (j + \frac{1}{2})$  specifies the partial wave,  $G_{\kappa}$  is the electron Green's function in the zeroth Hartree-Fock approximation and  $\Sigma_{\kappa}$  is the correlation potential in a given partial wave. Both are taken at zero electron energy. The physics of (6) is simple: the binding cannot take place unless the negative attractive correlation potential  $\hat{\Sigma}$  acquires a certain strength. As the integral (6) involves also the Hartree-Fock Green's function of the electron, it accounts for the fact that  $\hat{\Sigma}$  is added to the static ground state potential of the atom. It accounts for the Pauli principle as well: despite the fact that Eq. (1) usually has several eigenfunctions with large negative  $E_{\alpha}$ , corresponding to the closed orbitals of the atomic core, the magnitude of  $g_{\kappa}$  signals about the appearance of a *new* bound state in the spectrum.

As the above given criterion is only a necessary condition, it is interesting to estimate the actual magnitude of  $g_{\kappa}$  at which binding happens. In this paper we consider a number of bound and resonant states of an electron and a neutral atom. It enables us to check (6) for different partial waves. Besides that,  $g_{\kappa}$  is linear in  $\Sigma$ , and it is a convenient tool for comparing the role of different diagrams in Fig. 1.

The contributions of the direct and exchange diagrams to  $g_{\kappa}$  for the  $p$  and  $d$  waves in the Yb and Ra atoms are presented in Table II. As one can see from these data, the contribution of the exchange diagrams to the correlation potential is three to five times smaller than the contribution of the direct ones. It confirms that they do not need to be calculated with high numerical accuracy but they are by no means negligible. Forestalling the detailed discussion of Sec. III, note that only the  $p_{1/2}$  states are bound for both Yb and Ra, and for the Yb atom it is by a margin. Therefore one can expect a critical value of about 1.6 for  $g_{\kappa}$ . As will be shown in the next section, the values of  $g_{\kappa}$  indeed give a reliable indication of the

TABLE II. Contributions of the direct and exchange diagrams to  $g_{\kappa}$ .

| Atom | Wave      | Direct diagram<br>[Fig. 2(a)] | Exchange diagram<br>[Fig. 2(b)] | Sum  |
|------|-----------|-------------------------------|---------------------------------|------|
| Pd   | $s_{1/2}$ | 4.56                          | -0.56                           | 4.00 |
| Yb   | $p_{1/2}$ | 1.99                          | -0.36                           | 1.63 |
|      | $p_{3/2}$ | 1.73                          | -0.26                           | 1.47 |
|      | $d_{3/2}$ | 1.13                          | -0.19                           | 0.94 |
|      | $d_{5/2}$ | 1.08                          | -0.19                           | 0.89 |
| Ra   | $p_{1/2}$ | 2.93                          | -0.93                           | 2.00 |
|      | $p_{3/2}$ | 1.91                          | -0.46                           | 1.45 |
|      | $d_{3/2}$ | 1.61                          | -0.33                           | 1.28 |
|      | $d_{5/2}$ | 1.49                          | -0.33                           | 1.16 |

existence of a bound state or of a resonance. Thus it is a true measure of the correlation-potential strength.

Summarizing the above we can describe our method of calculation as follows:

- The Hartree-Fock-Dirac potential of the neutral atom  $\hat{V}^N$  and the Hamiltonian  $\hat{H}_0$  are used to generate a complete set of discrete (core) and continuous spectrum states for the many-body perturbation theory calculations of  $\hat{\Sigma}$ .
- The correlation potential  $\Sigma_{\kappa}(r_1, r_2, E_a)$  in the  $s$ ,  $p_{1/2}$ ,  $p_{3/2}$ ,  $d_{3/2}$ , and  $d_{5/2}$  partial waves is calculated within the second order in the residual Coulomb interaction. The most important direct diagrams are calculated using the Feynman diagram technique, whereas the exchange diagrams are calculated via direct summation over the intermediate states. Their contributions to the criterion (6) are estimated.
- Equation (1) is solved iteratively, starting from (4) for the bound state, or from the Hartree-Fock continuous spectrum state for the electron-scattering problem.

### III. RESULTS AND DISCUSSION

The procedure outlined above has been applied to investigate the interaction of the electron with the Pd, Ba, Yb, Hg, and Ra atoms. The results for the binding energies (electron affinities) and the energies of the low-lying resonances are presented in Table III together with the calculated values of  $g_{\kappa}$ .

As one can see from these data the inequality  $g_{\kappa} \gtrsim 1$  always means that there is either a bound state or a resonance at energy  $E < 0.5$  eV. Since  $g_{\kappa}$  measures the effect of the addition of the correlation potential to the static Hartree-Fock atomic field, these features are exclusively due to the correlation interaction of the electron with the atom. One can also notice that the condition  $g_{\kappa} \geq 1.6$  emerges as the *necessary and sufficient* condition for the existence of a bound state due to the correlation potential.

$\text{Pd}^-$  was the first among the stable negative ions formed by closed-shell atoms which had been calculated using the equation (1) [3]. The present calculation yields a binding energy of 0.54 eV for the  $\text{Pd}^- 4d^{10}5s$ . It is in good agreement with earlier calculations [8] and is remarkably close to the experimental value of 0.56 eV [12].

Unlike the alkaline-earth atoms and Yb, Pd has a very small polarizability. The  $s$ -wave binding of  $\text{Pd}^-$  takes place mainly because of the atom's unique  $4d^{10}$  ground state, and the extreme proximity of the  $5s$  subshell to the  $4d$  subshell: the lowest  $4d$ - $5s$  excitation energy in neutral Pd is only 0.814 eV [26]. This can also be understood by examining the magnitude of the scattering length  $a$  which governs the behavior of the  $s$ -wave phase shift at low electron energy:  $\delta = -ak$ ,  $k$  is the electron momentum. For the majority of closed-shell atoms the scattering length in the static Hartree-Fock approxima-

TABLE III. The binding energies, the energies of the low-lying electron resonances, and the parameters  $g_\kappa$  for the correlation-potential strength for the Pd, Ba, Yb, Hg, and Ra atoms. Comparison with experiments and other calculations.

| $Z$ | Atom              | Wave      | $g_\kappa$ | Energies (meV)   |                 | Other calculations or measurements  |
|-----|-------------------|-----------|------------|------------------|-----------------|---|
|     |                   |           |            | Binding          | Resonant        |   |
| 46  | Pd $4d^{10}$      | $s_{1/2}$ | 4.00       | 540              |                 | 560 <sup>a</sup> 140 <sup>b</sup> 525 <sup>c</sup>                                      |
| 56  | Ba $5p^6 6s^2$    | $p_{1/2}$ | 2.43       | 190              |                 | 192 <sup>c</sup> 176 <sup>d</sup> 144 <sup>b</sup><br>148 <sup>e</sup> 199 <sup>f</sup> |
|     |                   | $p_{3/2}$ | 2.08       | 133              |                 |   |
|     |                   | $d_{3/2}$ | 1.60       | 15               |                 |   |
|     |                   | $d_{5/2}$ | 1.54       |                  | 60              | 210 <sup>b</sup>  |
| 70  | Yb $4f^{14} 6s^2$ | $p_{1/2}$ | 1.63       | 36               |                 | 54 <sup>f</sup> 98.5 <sup>b</sup>   |
|     |                   | $p_{3/2}$ | 1.47       |                  | 30              |   |
|     |                   | $d_{3/2}$ | 0.94       |                  | 1500            |   |
|     |                   | $d_{5/2}$ | 0.89       |                  | 1600            |   |
| 80  | Hg $5d^{10} 6s^2$ | $p_{1/2}$ | 0.93       |                  | 230             | 630 <sup>h</sup>  |
|     |                   | $p_{3/2}$ | 0.71       |                  | 540             | 630 <sup>h</sup>  |
|     |                   | $d_{3/2}$ | 0.24       |                  |                 |   |
|     |                   | $d_{5/2}$ | 0.24       |                  |                 |   |
| 88  | Ra $6p^6 7s^2$    | $p_{1/2}$ | 2.00       | 148 <sup>g</sup> |                 | 75 <sup>d</sup> 125 <sup>f</sup>  |
|     |                   | $p_{3/2}$ | 1.45       |                  | 18 <sup>g</sup> |   |
|     |                   | $d_{3/2}$ | 1.28       |                  | 330             |   |
|     |                   | $d_{5/2}$ | 1.16       |                  | 440             |   |

<sup>a</sup>Experiment [12].

<sup>b</sup>Nonrelativistic Dyson equation method [3,4,15,28,29].

<sup>c</sup>Relativistic Dyson equation method [8].

<sup>d</sup> $R$ -matrix approach [7].

<sup>e</sup>Multiconfigurational Hartree-Fock [6].

<sup>f</sup>Local density functional method [5,14].

<sup>g</sup>Relativistic correlation potential method [10,16].

<sup>h</sup>Experiment [17].

tion is positive. It becomes negative due to the correlation potential producing the Ramsauer-Townsend effect (see, e.g., [27] for noble-gas atoms and [28], [29] for alkaline-earth atoms). In contrast, the scattering length for Pd is already negative in the Hartree-Fock-Dirac approximation:  $a = -10$  a.u. It indicates the existence of a virtual level at  $\hbar/2a^2 \simeq 0.14$  eV energy. That is why a relatively weak electron-Pd correlation potential is capable of forming quite a strongly bound  $s$  state. It is interesting to note that the nonrelativistic value of  $a$  is about two times smaller:  $a = -4.5$  ( $\hbar/2a^2 \simeq 0.67$  eV). So, the relativistic effects are very important in forming the Pd<sup>-</sup> negative ion and the neglect of them seems to be the main reason for the underestimation of the electron affinity in [3].

A joint consideration and comparison of binding properties of the Ba, Yb, and Ra atoms provides a clear insight into the role of the correlation interaction and relativistic effects. Ba and Ra are the heaviest alkaline-earth atoms and Yb differs from Ba by the presence of the compact  $4f^{14}$  subshell. The outermost subshell for these atoms is  $ns^2$ . Based on the values of their polarizabilities one would expect correlation potentials of similar strength for Ba and Ra, and a smaller one for Yb. On the other hand, the relativistic effects, and in particular, the spin-orbit interaction, are increasing successively

from Ba to Ra. The combined action of these factors produces the following picture. The lowest state  $p_{1/2}$  is bound for all three atoms, forming the ground states of the ions: Ba<sup>-</sup>  $6s^2 6p$ , Yb<sup>-</sup>  $4f^{14} 6s^2 6p$ , and Ra<sup>-</sup>  $7s^2 7p$ . The binding energy for Yb<sup>-</sup> is considerably lower than those for Ba and Ra. Its magnitude is 36 meV, which is within the error bars of [14]  $54 \pm 27$  meV. It also agrees with the experiment [13], which provides the lower limit of 10 meV for it.

The effect of the spin-orbit interaction is already quite marked in Ba: the fine-structure interval  $\Delta E_{fs} = 57$  meV constitutes 30% of the electron affinity. This value coincides with our earlier estimation based on  $Z^2$  dependence of the fine-structure interval [10]. In Yb as well as in Ra (see also [10]) the spin-orbit  $p_{1/2}$ - $p_{3/2}$  splitting becomes larger than the electron affinity. The  $p_{3/2}$  state of the negative ion exists as a quasistationary state in the continuum. It manifests itself in the resonant behavior of the  $p_{3/2}$  phaseshift (Fig. 5), and produces a large, sharp maximum in the scattering cross section (Fig. 6). The energies of the resonances given in Table III correspond to the maximum in the partial wave cross section.

The interaction of the  $d$ -wave electrons with Ba, Yb, and Ra is also very peculiar. In contrast with previous *ab initio* [28,29] and model potential [16,19] calculations the energies of the  $d_{3/2}$ ,  $d_{5/2}$  states of Ba turned out to

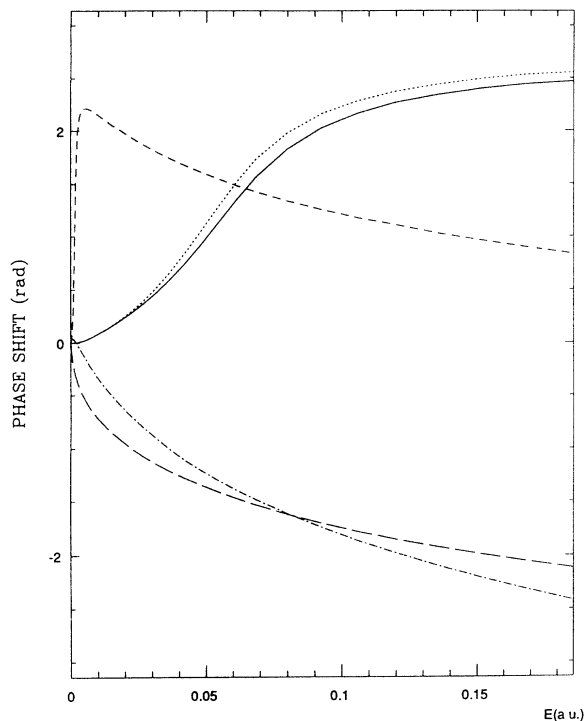


FIG. 5. Dependence of  $s$  (dot-dash curve),  $p_{1/2}$  (long dash),  $p_{3/2}$  (short dash),  $d_{3/2}$  (dot),  $d_{5/2}$  (solid curve) phases on energy for Yb.

be very close to zero. In fact the lower  $d_{3/2}$  state in our calculation is weakly bound, and the upper  $d_{5/2}$  resonant state has much smaller energy than that of a  $d$  resonance in [28].

It is necessary to recall here that we estimate the accuracy of the second-order calculation of the correlation potential as several per cent. For the case of  $d$  states of  $\text{Ba}^-$  the corresponding uncertainty in the calculated positions of the energy levels is about 30–60 meV. It

does not allow us to prove or disprove the existence of the bound  $6s^2 5d_{3/2}$  state of  $\text{Ba}^-$ . However, the energies obtained indicate that the positions of the  $d$  resonances for electron scattering by the Ca, Sr, and Ba atoms may be substantially lower than those calculated in [28,29]. This supposition agrees with the fact that the measured electron-alkaline-earth atom scattering cross sections [30] exhibit the  $d$ -wave resonance for Ca at 0.78 eV (instead of 1.44 eV in [28]), and do not show any resonant features for Sr at  $E > 0.09$  eV (in contrast with the prediction of the  $d$  resonance at 0.87 eV [28]).

In the Yb and Ra atoms the  $d$  states have much higher energies than in Ba. Thus their resonant character does not raise any doubt, even at the present level of accuracy, of the correlation-potential calculation.

The abrupt dependence of the resonant  $p$  and  $d$  phase-shifts on energy together with the strong spin-orbit interaction produces a phenomenon of near 100% spin polarization of the scattered electrons in the large energy interval near the resonance and at appropriate scattering angle ( $\simeq 90^\circ$  for  $p$  resonances and  $\simeq 54^\circ$  and  $\simeq 125^\circ$  for  $d$  resonances) (see [16] for more detailed discussion). It is illustrated in Fig. 7, where the polarization  $P$  and the differential cross section for electrons scattered by Yb are shown as functions of the scattering angle  $\theta$ . In principle the analogous effects can be observed in the vicinity of all resonances listed in Table III. However, most of them have very small energies, which makes the effect difficult to detect experimentally.

We suppose that Hg atoms may be the best for the observation of the low-energy electron spin polarization. According to the experimental data [17] there is a prominent  $p$  resonance at  $E = 0.63$  eV with width  $\Gamma \sim 0.4$  eV. The calculations show that the Hg atom does not form stable negative-ion states, its polarizability being much smaller than those of Ba, Yb, and Ra. Nevertheless, the electron-Hg correlation potential forms resonant  $p_{1/2}$  and  $p_{3/2}$  states (see the phase shifts in Fig. 8). The elastic cross section has a broad asymmetric maximum associated with them (Fig. 9). The position of the maximum

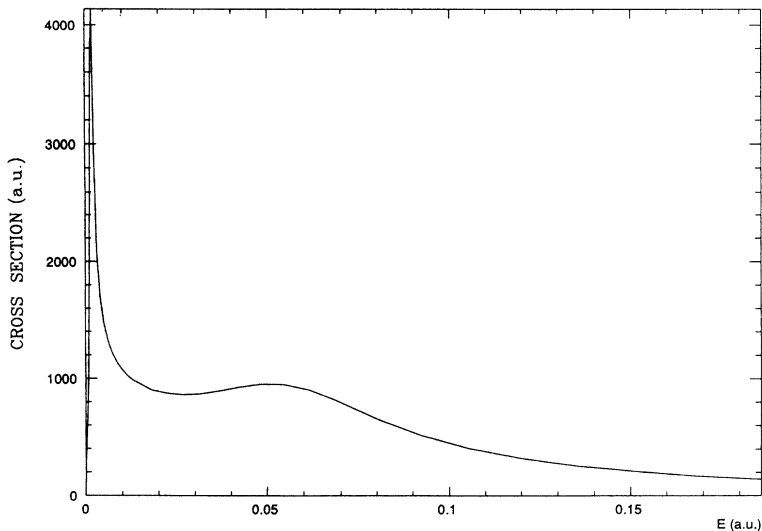


FIG. 6. Total cross section for Yb as a function of energy.

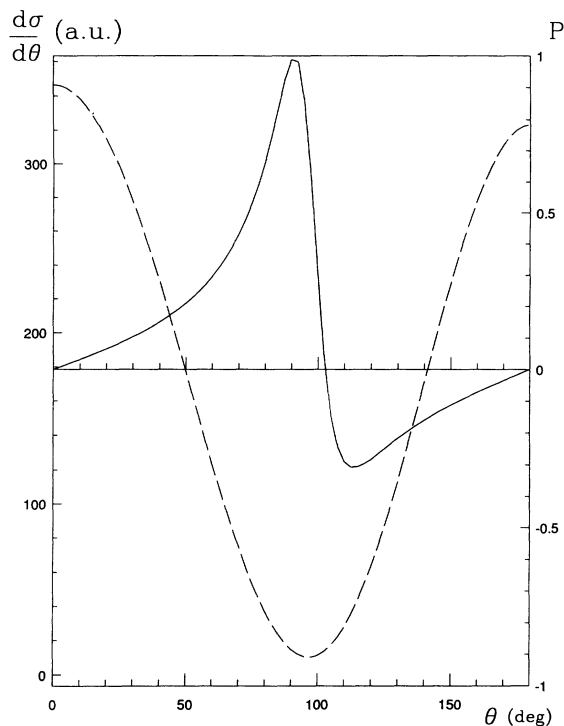


FIG. 7. Differential cross section (dashed curve) and polarization of scattered electrons (solid curve) for Yb at  $E = 0.19$  eV.

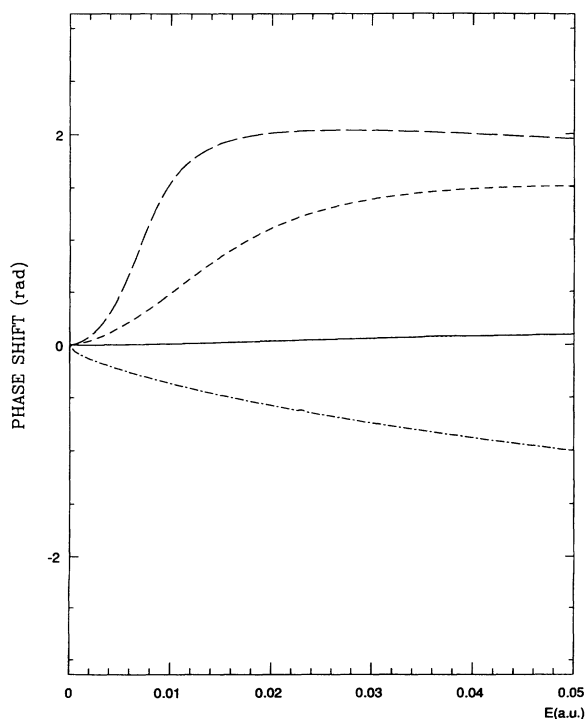


FIG. 8. Dependence of  $s$  (dot-dash curve),  $p_{1/2}$  (long dash),  $p_{3/2}$  (short dash), and  $d$  (solid curve) phases on energy for Hg.

appears to be considerably lower and its width is larger than the experimental values. Making this comparison one should bear in mind the strong asymmetry of the peak, which might hinder precise determination of the resonance parameters by the transmitted current technique [17]. Figures 10 and 11 show the spin polarization parameters for Hg at  $E = 0.3$  and  $E = 0.5$  eV. The large widths and separation of the  $p_{1/2}$  and  $p_{3/2}$  resonances enable one to observe a high degree of spin polarization over the extended range of electron energies.

Summarizing, we observe that the atoms considered above, as well as some other closed-shell atoms, display very peculiar properties in the interaction with low-energy electrons. They include negative-ion bound states and resonances formed due to the strong correlation electron-atom interaction. The strength of this interaction can be measured for each partial wave with the help of the criterion we propose. In some cases (Ba,  $d$  wave) it requires a very accurate calculation of the correlation potential to determine the actual character of such states. The relativistic spin-orbit interaction produces strong spin polarization of the electrons scattered by spherically symmetric target at certain angles. The mercury atom is probably the best candidate to observe this effect experimentally.

#### ACKNOWLEDGMENTS

One of us (G.F.G.) would like to thank M. Yu. Kuchiev and O. P. Sushkov for useful discussions concerning the proposed criterion, and V. V. Flambaum who suggested the derivation of the criterion for the low-lying resonant state.

#### APPENDIX: THE NECESSARY CONDITION FOR THE EXISTENCE OF A NEGATIVE-ION BOUND STATE

The aim of the Appendix is to derive the criterion (6), which estimates the capacity of a nonlocal potential  $\hat{\Sigma}$  added to a zero-order Hamiltonian  $\hat{H}_0$  to create an extra bound state. Since the whole paper concerns the problem of the interaction of an electron with an atom we will consider this particular case hereafter. However, the criterion itself is a mathematical statement: it may be proved with more rigor, as well as applied to other problems.

The behavior of the electron in the field of the closed-shell atom is described by the equation

$$\hat{H}_0\psi(\mathbf{r}) + \int \Sigma(\mathbf{r}, \mathbf{r}')\psi(\mathbf{r}')d\mathbf{r}' = \epsilon\psi(\mathbf{r}), \quad (\text{A1})$$

where  $\hat{H}_0$  is the Hartree-Fock Hamiltonian, and  $\Sigma(\mathbf{r}, \mathbf{r}')$  is the correlation potential, represented in the leading order by the diagrams in Fig. 1. The spectrum of  $\hat{H}_0$

$$\hat{H}_0\varphi_\nu(\mathbf{r}) = \epsilon_\nu\varphi_\nu(\mathbf{r}) \quad (\text{A2})$$

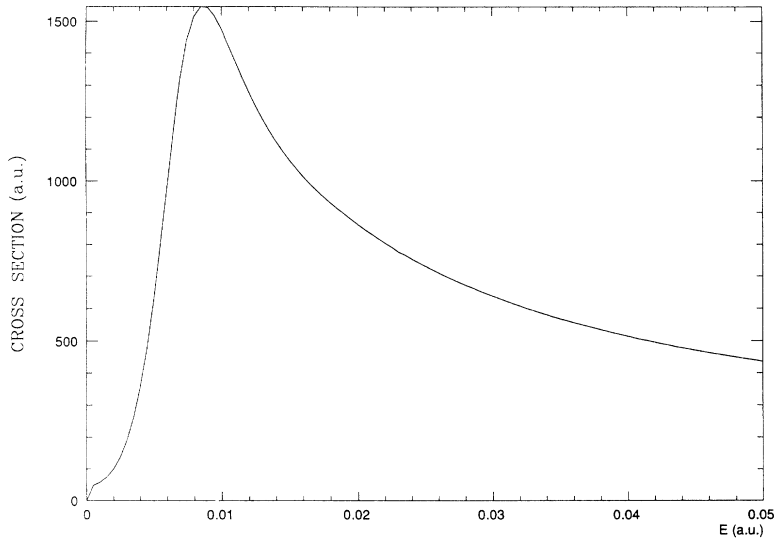


FIG. 9. Total cross section for Hg as a function of energy.

contains the discrete states  $\nu \leq F$  occupied in the atomic ground state ( $F$  denotes the Fermi level), and the excited states  $\nu > F$ , representing the motion of an extra electron in the “frozen” Hartree-Fock field of the atomic core. The Hartree-Fock potential of the neutral atom is a short-range one, and is too weak to bind the additional electron. The main question then is as follows: is the spectrum of (A1) different from that of (A2), having an additional bound state of the negative ion?

Expanding  $\psi$  in terms of the complete set of  $\varphi_\nu$  states of  $H_0$

$$\psi(\mathbf{r}) = \sum_{\nu} C_{\nu} \varphi_{\nu}(\mathbf{r}), \quad (\text{A3})$$

$$C_{\nu} = \int \varphi_{\nu}^*(\mathbf{r}) \psi(\mathbf{r}) d\mathbf{r} \quad (\text{A4})$$

one obtains Eq. (A1) in matrix form:

$$\epsilon_{\nu} C_{\nu} + \sum_{\nu'} \langle \nu | \Sigma | \nu' \rangle C_{\nu'} = \epsilon_0 C_{\nu}. \quad (\text{A5})$$

Since the operator  $\hat{H}_0 + \hat{\Sigma}$  is spherically symmetric its eigenfunctions have definite angular momentum, and both the expansion coefficients  $C_{\nu}$  and the equation (A5) can be written for a partial wave of interest. It means that  $\sum_{\nu}$  includes the summation over the core orbitals in this partial wave and the integration over the energies of the continuum.

Suppose a loosely bound state  $\epsilon_0 < 0$  emerges in the spectrum of (A1) and (A5) due to  $\hat{\Sigma}$ . If the binding energy  $|\epsilon_0|$  is small, the wave function  $\psi$  is very much delocalized, and has a radius much greater than that of the atomic core. It makes the contribution of the core orbitals to the sum in (A3) negligibly small. Then only the continuous spectrum states  $\nu$  need to be taken into account in (A5). One can justify it in another way. Solving the eigenvalue problem for the  $\delta_{\nu\nu'} + \langle \nu | \Sigma | \nu' \rangle$  matrix, we have a few large negative eigenvalues corresponding to the occupied core orbitals. They are very close to the

Hartree-Fock energies  $\epsilon_{\nu}$  ( $\nu \leq F$ ), and the submatrix  $\nu, \nu' \leq F$  is very weakly coupled to the rest of the matrix, so that one can omit it in the calculation of the other eigenvalues. The new bound state, provided it appears in the spectrum of (A5), is then the lowest one, and can be found from the variational principle

$$\epsilon_0 = \min \left\{ \sum_{\nu, \nu'} (\epsilon_{\nu} \delta_{\nu, \nu'} + \langle \nu | \Sigma | \nu' \rangle) C_{\nu} C_{\nu'} \right\}, \quad (\text{A6})$$

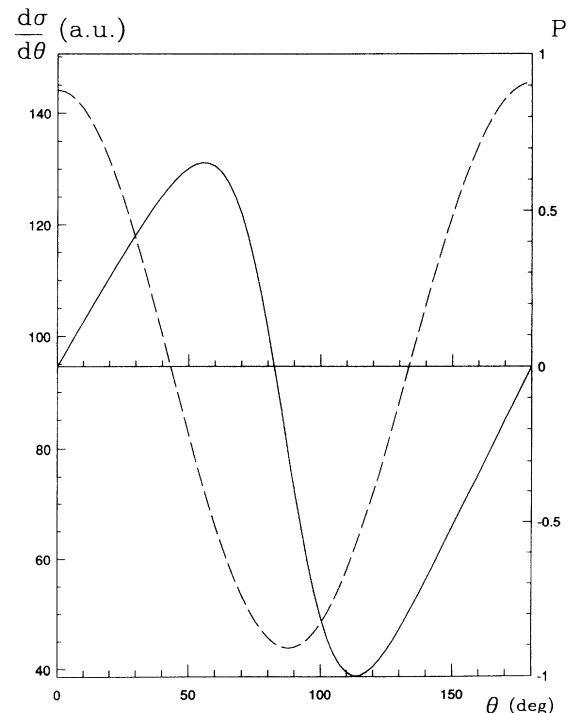


FIG. 10. Differential cross section (dashed curve) and polarization of scattered electrons (solid curve) for Hg at  $E = 0.30$  eV.



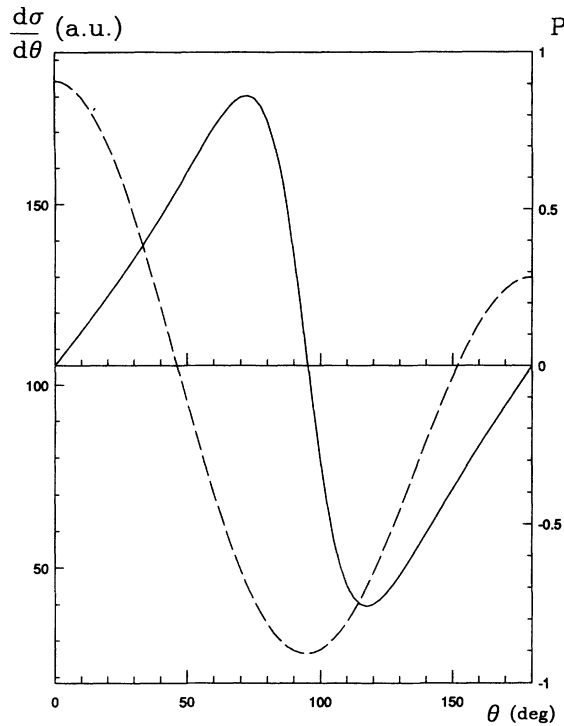


FIG. 11. Differential cross section (dashed curve) and polarization of scattered electrons (solid curve) for Hg at  $E = 0.50$  eV.

restricted by the normalization condition  $\sum_{\nu} C_{\nu}^2 = 1$ . The basis functions  $\varphi_{\nu}$  can always be chosen so that the  $C_{\nu}$  are real, and  $C_{\nu}^* = C_{\nu}$ , as supposed above.

Let us now find a matrix operator  $B_{\nu\nu'}$  to be used in (A5) in place of  $\langle\nu|\Sigma|\nu'\rangle$ , for which the equation is solved analytically. This is a so called separable potential  $B_{\nu\nu'} = -f_{\nu}f_{\nu'}$ , where the minus sign means attraction. The equation

$$\epsilon_{\nu}C_{\nu} - \sum_{\nu'} f_{\nu}f_{\nu'}C_{\nu'} = \epsilon_0C_{\nu} \quad (\text{A7})$$

then yields

$$\sum_{\nu} \frac{f_{\nu}^2}{\epsilon_0 - \epsilon_{\nu}} = -1. \quad (\text{A8})$$

The summation in (A8) runs over the continuous spectrum of  $\epsilon_{\nu} > 0$ . It is easy to check that the condition

$$\sum_{\nu} \frac{f_{\nu}^2}{\epsilon_{\nu}} > 1 \quad (\text{A9})$$

is necessary and sufficient for (A8) to have a negative root, and, consequently, for (A7) to have a negative eigenvalue  $\epsilon_0$ .

One may specify the auxiliary separable potential, setting its diagonal matrix elements equal to those of  $\hat{\Sigma}$ :

$$B_{\nu\nu} \equiv \langle\nu|\Sigma|\nu\rangle, \quad \text{or} \quad f_{\nu} = (-\langle\nu|\Sigma|\nu\rangle)^{1/2}. \quad (\text{A10})$$

It will be shown below that  $B_{\nu\nu'}$  thus defined is stronger than  $\langle\nu|\Sigma|\nu\rangle$ , i.e., the lowest eigenvalue of the former is lower than that of the latter. Then the condition (A9) applied to this  $B_{\nu\nu'}$  becomes a necessary condition for the existence of a bound state for  $\langle\nu|\Sigma|\nu\rangle$ . It reads as

$$-\sum_{\nu} \frac{\langle\nu|\Sigma|\nu\rangle}{\epsilon_{\nu}} > 1. \quad (\text{A11})$$

Note that the left hand side is  $Sp(\hat{G}\hat{\Sigma})$ , where  $\hat{G}$  is the electron Green's function for (A2):  $\hat{G} = \sum_{\nu} \frac{|\nu\rangle\langle\nu|}{E - \epsilon_{\nu}}$  calculated at  $E = 0$ . Then one may rewrite (A11) in the coordinate representation:

$$\int G_{\kappa}(r', r)\Sigma_{\kappa}(r, r')dr dr' > 1. \quad (\text{A12})$$

Here  $\kappa$  denotes the partial wave, and both the Green's function and the correlation potential are calculated at zero energy.

To show that the above constructed  $B_{\nu\nu'}$  is stronger than  $\langle\nu|\Sigma|\nu\rangle$ , let us note first that for the lowest eigenstate  $C_{\nu}$  as a function of continuous variable  $\nu$  does not have nodes. The property necessary then follows from the variational principle (A6), if one supposes that

$$-f_{\nu}f_{\nu'} \leq \langle\nu|\Sigma|\nu'\rangle. \quad (\text{A13})$$

Let us prove this inequality for the case when the correlation potential is given by the diagram 1(a), or more precisely, when one can write down the second-order like expression

$$\langle\nu|\Sigma|\nu'\rangle = \sum_{\alpha} \frac{\langle\nu|V|\alpha\rangle\langle\alpha|V|\nu'\rangle}{E - E_{\alpha} + i\delta}, \quad (\text{A14})$$

where  $V$  is the residual interaction,  $\alpha$  denotes the intermediate state [two particles and a hole in Fig. 1(a)],  $E_{\alpha}$  is its energy, which is greater than the lowest excitation energy of the atom, and  $E$  is the energy at which  $\hat{\Sigma}$  is calculated. Searching for a bound state, one should aim at  $E = \epsilon_0 < 0$ . This means that the diagonal matrix element  $\langle\nu|\Sigma|\nu\rangle$  is negative, and the definition (A10) is correct. It is also seen from (A14) that the closer the energy  $E < 0$  to zero, the stronger is the attraction produced by  $\hat{\Sigma}$ . If  $\hat{\Sigma}$  calculated at  $E = 0$  does not produce a bound state, then it does not exist at all. This justifies the use of the correlation potential calculated at zero energy in condition (A12).

The expression (A14) at  $E = 0$  can be written as follows:

$$\langle\nu|\Sigma|\nu'\rangle = -\sum_{\alpha} g_{\nu}(\alpha)g_{\nu'}(\alpha),$$

$$\text{where } g_{\nu}(\alpha) \equiv \langle\nu|V|\alpha\rangle/\sqrt{E_{\alpha}}. \quad (\text{A15})$$

Then

$$f_{\nu}f_{\nu'} = \left(\sum_{\alpha} g_{\nu}(\alpha)g_{\nu'}(\alpha)\right)^{1/2} \left(\sum_{\beta} g_{\nu'}(\beta)g_{\nu}(\beta)\right)^{1/2}, \quad (\text{A16})$$

and (A13) immediately follows from the Cauchy-Schwartz inequality.

It should be noted that in the simplest possible case when  $H_0$  is the nonrelativistic Hamiltonian of a free particle and  $\hat{\Sigma}$  is local, so that  $\Sigma(\mathbf{r}, \mathbf{r}') = \delta(\mathbf{r} - \mathbf{r}')U(r)$  [ $U(r) < 0$  is an attractive potential], the criterion turns into the well known Bargman formula [21]

$$2 \int r |U(r)| dr \geq 2l + 1, \quad (\text{A17})$$

where  $l$  is the orbital momentum of the partial wave. In obtaining (A17) we used the expression for the free particle Green's function and correlation potential in the  $l$ th partial wave:  $G_l(r, r') = -\frac{2}{2l+1} r_{<}^{l+1}/r_{>}^l$ ,  $\Sigma_l(r, r') = U(r)\delta(r - r')$ . The particle's mass is set to 1.

There is an interesting case where the condition (A12) turns into an exact necessary and sufficient one. Suppose there is a low-lying resonant state in the spectrum of the zero-order Hamiltonian. Then the Green's function at

small  $E$  is represented by a contribution of the nearby pole:  $G_\kappa(r, r') \simeq \varphi_0(r)\varphi_0(r')/(E - E_0)$ . Here  $E_0 > 0$  is the real part of the energy of the resonance and  $\varphi_0(r)$  is the normalized radial function of this quasistationary state ([31]). We suppose that its width is small:  $\Gamma \ll E_0$ . This is true for the resonances with  $l \geq 1$  if  $E_0$  is small enough. Introducing this Green's function into (A12) one obtains  $E_0 + \langle \varphi_0 | \Sigma_\kappa | \varphi_0 \rangle < 0$ . It is apparently a perturbation theory result, which is valid because only a small additional potential  $\hat{\Sigma}$  is required to turn the resonant state into the bound one.

Apart from the "electron plus atom" problem, one may apply (A12) to investigate the interaction of atoms with positrons. In this case the correlation potential overpowers the static repulsion between the atom and the positron, and it may give birth to a bound or a resonant state [32], especially for heavy atoms with large dipole polarizabilities. The above given derivation looks even more rigorous for the positron, as there are no deep core bound states, and the possible weakly bound state is indeed the lowest one.

- 
- [1] C. Froese Fischer, J. B. Lagowski, and S. H. Vosko, *Phys. Rev. Lett.* **59**, 2263 (1987).
- [2] D. J. Pegg, J. S. Thompson, R. N. Compton, and G. D. Alton, *Phys. Rev. Lett.* **59**, 2267 (1987).
- [3] L. V. Chernysheva, G. F. Gribakin, V. K. Ivanov, and M. Yu. Kuchiev, *J. Phys. B* **21**, L419 (1988).
- [4] G. F. Gribakin, B. V. Gul'tsev, V. K. Ivanov, and M. Yu. Kuchiev, *Pis'ma Zh. Tekh. Fiz.* **15**, 32 (1989) [*Sov. Tech. Phys. Lett.* **15**, 468 (1989)].
- [5] S. H. Vosko, J. B. Lagowski, and I. L. Mayer, *Phys. Rev. A* **39**, 446 (1989).
- [6] C. Froese Fischer, *Phys. Rev. A* **39**, 963 (1989).
- [7] L. Kim and C. H. Greene, *J. Phys. B* **22**, L175 (1989).
- [8] W. R. Johnson, J. Sapirstein, and S. A. Blundell, *J. Phys. B* **22**, 2341 (1989).
- [9] G. F. Gribakin, B. V. Gul'tsev, V. K. Ivanov, and M. Yu. Kuchiev, *J. Phys. B* **23**, 4505 (1990).
- [10] V. A. Dzuba, V. V. Flambaum, G. F. Gribakin, and O. P. Sushkov, *Phys. Rev. A* **44**, 2823 (1991).
- [11] M. A. Garwan, L. R. Kilius, A. E. Litherland, M.-J. Nadeau, and X.-L. Zhao, *Nucl. Instrum. Methods B* **52**, 512 (1990).
- [12] C. S. Feigerle, R. R. Corderman, S. V. Bobashev, and W. C. Lineberger, *J. Chem. Phys.* **74**, 1580 (1981).
- [13] A. E. Litherland, L. R. Kilius, M. A. Garwan, M.-J. Nadeau, and X.-L. Zhao, *J. Phys. B* **24**, L233 (1991).
- [14] S. H. Vosko, J. A. Chevvarly, and I. L. Mayer, *J. Phys.* **24**, L225 (1991).
- [15] A. A. Gribakina, G. F. Gribakin, and V. K. Ivanov, *Phys. Lett. A* **168**, 280 (1992).
- [16] V. A. Dzuba, V. V. Flambaum, and O. P. Sushkov, *Phys. Rev. A* **44**, 4224 (1991).
- [17] P. D. Burrow, J. A. Michejda, and J.-J. Comer, *J. Phys. B* **9**, 3225 (1976).
- [18] J. Yuan and Z. Zhang, *Phys. Lett. A* **160**, 81 (1991).
- [19] J. Yuan and Z. Zhang, *Phys. Lett. A* **168**, 291 (1992).
- [20] K. D. Sen, P. C. Schmidt, and A. Weiss, *Theor. Chim. Acta* **58**, L69 (1980). S. G. Bratsch, *Chem. Phys. Lett.* **98**, 113 (1983).
- [21] V. Bargman, *Proc. Natl. Acad. Sci. U.S.A.* **38**, 961 (1952).
- [22] V. A. Dzuba, V. V. Flambaum, P. G. Silvestrov, and O. P. Sushkov, *J. Phys. B* **20**, 1399 (1987).
- [23] V. A. Dzuba, V. V. Flambaum, and O. P. Sushkov, *Phys. Lett. A* **140**, 493 (1989).
- [24] *CRC Handbook of Chemistry and Physics* (CRC, Boca Raton, 1989).
- [25] Our RPA calculation yields a value of  $\alpha \simeq 22$  a.u., and it is consistent with the photoionization cross sections of M. Ya. Amusia and N. A. Cherepkov, *Case Stud. At. Phys.* **5**, 47 (1975); V. Radojevic and W. R. Johnson, *J. Phys. B* **16**, 177 (1983).
- [26] A. A. Radtsig and B. M. Smirnov, *Parameters of Atoms and Atomic Ions: Handbook* (Moscow, Energoatomizdat, 1986).
- [27] M. Ya. Amusia, N. A. Cherepkov, L. V. Chernysheva, S. G. Shapiro, and A. Tancic, *Zh. Eksp. Teor. Fiz.* **68**, 2023 (1975) [*Sov. Phys. JETP* **41**, 1012 (1975)].
- [28] G. F. Gribakin, V. K. Ivanov, and M. Yu. Kuchiev, in *Proceedings of the XI All-Union Conference on Physics of Electron and Atomic Collision, Cheboksary, 1991*, edited by A. L. Orbeli (A.F. Ioffe PTI, Leningrad, 1991).
- [29] G. F. Gribakin, B. V. Gultsev, V. K. Ivanov, M. Yu. Kuchiev, and A. R. Tancic, *Phys. Lett. A* **164**, 73 (1992).
- [30] N. I. Romanuk, O. B. Shpenik, and I. p. Zapesochny, *Zh. Eksp. Teor. Fiz. Pis'ma* **32**, 472 (1980) [*JETP Lett.* **32**, 452 (1980)].
- [31] A. I. Baz, Ya. B. Zeldovich, and A. M. Perelomov, *Scattering, Reactions and Decays in the Nonrelativistic Quantum Mechanics* (Moscow, Nauka, 1971).
- [32] V. A. Dzuba, V. V. Flambaum, W. A. King, B. N. Miller, and O. P. Sushkov, *Phys. Scr.* **T46**, 248 (1993).